A Numerical Study of Heating, Mixture Formation and Detailed Combustion Around a Fuel Droplet Under Engine-Like Conditions

P.Stapf, R.R.Maly, H.A.Dwyer* and J.Warnatz**

Daimler-Benz AG
Aero- and Thermodynamics, FIM/T, Code G206
D-70546, Stuttgart
Germany
* *University of California*
** *University of Stuttgart*

ABSTRACT

Fundamentals of Diesel combustion are studied by a detailed one-dimensional computational model, in which the fuel spray is represented by a characteristic volume element containing only a single droplet. The various interactions between the numerous droplets in a fuel spray are simulated by incorporating additionally the gaseous components and/or radicals into the turbulent gas flow around the representative droplet. Both fluid dynamics and reaction kinetics are treated explicitly. Thus the model permits detailed investigations of the controlling physical and chemical processes with high spatial resolution and highly detailed reaction kinetics without the limitations imposed by the multi-body problems of a full spray. At present two liquid components can be handled, whereas the number of gaseous species is merely limited by capacity and speed of the computer system used. In this study methanol was chosen as a model fuel for studying droplet heating, vaporization, mixing, ignition, combustion and pollutant formation.

INTRODUCTION

A full physical and chemical calculation of the properties of spray combustion is still not possible on current computers although this is needed to enable sensible reductions in fuel consumption and raw emissions of Diesel engines to be made. This is possible, however, if the spray is represented by a characteristic spray element of dimension L = mean droplet separation containing a single droplet with r = mean droplet size (for details of the definition see Fig. 1). In this study we have chosen this approach using a single methanol droplet in an appropriate engine-like environment for this purpose. Heating and vaporization of the droplet are based on a detailed description of heat and mass transfer between liquid and gas phases. Detailed reaction kinetics are used in the gas phase to model ignition, combustion and pollutant formation. To reduce the complexity of these processes and their interactions still further spherical symmetry is assumed so that a one-dimensional model can be applied without loosing the general validity [1,2]. To corroborate this model the calculated ignition delay times will be compared to engine results.

COMPUTATIONAL MODEL

The model is based on a control volume formulation published earlier [3]. General transport equations are used both for the liquid and the gas phase. They are solved simultaneously for the liquid droplet and the surrounding gas atmosphere. The liquid is assumed to be a non-reacting mixture also in case two liquid components are considered. For the gas phase detailed chemistry [4-7] is included into the set of equations being solved simultaneously with the flow equations, i.e. continuity, momentum, energy and species conservation [3,8].

Reactions in the gas phase are treated in 2 ways: (1) for detailed reaction kinetic calculations the CHEMKIN code [9] is invoked and for (2) overview runs (Fig. 2) simple but fast semi-empirical correlations are used [10]:

$$Fuel + n_1\, O_2 \rightarrow n_2\, CO_2 + n_3\, H_2O$$

where

$$k = A T^n \exp(-E_a/RT)\, [Fuel]^a [Oxidizer]^b$$

with reaction rate k, pre-exponential factor A, temperature T, activation energy E_a, gas constant R.

The properties of the liquid fluids are described by semi-empirical correlations accounting for the droplet temperature during the heat-up process [11,12]. The heat of vaporization affects strongly the energy balance at the droplet surface and must be treated in detail. The heat of vaporization ΔH_{vb} (J/mol) is evaluated at reference conditions ($T = T_b$, pressure p=1.01 bar) [11]:

$$\Delta H_{vb} = 1.093 R T_c \left[\frac{T_b}{T_c} \cdot \frac{\ln p_c - 1.013}{0.93 - T_b/T_c} \right] \qquad (1)$$

where T_b=boiling temperature, T_c=critical temperature, p_c=critical pressure. The actual temperature is normalized to T_b, thus:

$$\Delta H_v = \Delta H_{vb} \left(\frac{1 - T/T_c}{1 - T_b/T_c} \right)^{0.38} \qquad (2)$$

The vapor pressure p_{vp} of methanol is given by the correlation function [11]:

$$\ln\frac{p_{vp}}{p_c} = \frac{c_1\tau + c_2\tau^{1.5} + c_3\tau^3 + c_4\tau^6}{T/T_c} \tag{3}$$

with $\tau = 1 - T/T_c$, c_1=-8.54796, c_2=0.76982, c_3=-3.10850, c_4=1.54481.

The heat capacity of the liquid, c_{pl} (J/mol.K), is calculated temperature dependent [11]. Reference values for c_p^0 are tabulated in [13], and ω = 0.556 [11]:

$$\frac{c_{pl} - c_p^0}{R} = 1.45 + 0.45(1 - T/T_c)^{-1} + 0.25\omega\left[17.11 + 25.2(1 - T/T_c)^{1/3}(T/T_c)^{-1} + 1.742(1 - T/T_c)^{-1}\right] \tag{4}$$

The thermal conductivity of the liquid, λ_l (W/m.K), is derived from a temperature dependent correlation [11]:

$$\lambda_l = \frac{\left(1.11/M^{1/2}\right)\left[3 + 20(1 - T/T_c)^{2/3}\right]}{3 + 20(1 - T_b/T_c)^{2/3}} \tag{5}$$

with M = molecular weight, g/mol.

The transport equations for liquid and gas phase, resp., are coupled at the interface between liquid and gas with a set of equations, which describes the forces, the heat and the mass transfer between droplet and gaseous environment. The boundary equations are derived by a zero volume approach of the control volume [3,8]. For the physical setup of these equations, dynamic equilibrium at the interface is assumed, i.e. the energy flux from the gas phase is used for heating and vaporizing the droplet.

Since the droplet is assumed to remain spherical during the injection and combustion process, the originally three-dimensional problem is reduced to a one dimensional one. Thus a concentric, geometrically stretched grid is used with an extremely high spatial resolution on both sides of the interface between liquid and gas phase to resolve details and to provide high accuracy of the results. To maintain this fine resolution also during vaporization and expansion of the vapor cloud around the droplet, this grid has been fixed to the position of the interface. Therefore, an additional equation is included into the transport equations describing this moving boundary:

$$\frac{\partial}{\partial t}\left[\iiint_{\Omega} dV\right] = \iint_{S} v_b\, dA\,. \tag{6}$$

Finally engine conditions are introduced into this model by appropriately prescribed polytropic, time dependent changes in pressure and temperature of the gas phase which are derived from engine experiments as well as flow data from the spray edge. Thus the effects of piston motion and injection on the combustion process around the droplet is realistically simulated as well. A schematic of the spray element is shown in Fig.1 indicating the parameters which can be varied.

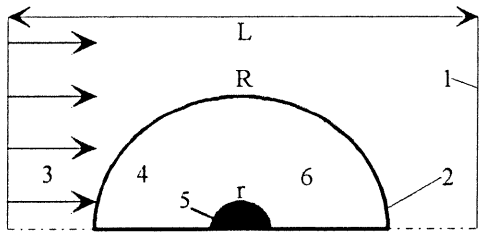

Fig. 1 Definition of the spray element (1), half section: L = mean droplet separation in the spray, R ≥ 10r, r = mean droplet radius, computational domain (2), the incoming gas flow (3) mimics the effects of the spray properties upstream of the droplet (flow velocity, air, fuel vapor, radicals, products, pollutants), interacts with the droplet (5) = liquid phase (binary fuel mixture, r, T_d, ΔH_v, c_{pl}, λ_l) and produces unburned (4) and burned (6) mixtures (T_g, p_g, air, fuel vapor, radicals, mixing, ignition, combustion, products, pollutants, detailed or global kinetics).

RESULTS

Unless specified differently, test calculations have been carried out for the conditions summarized in Table 1. These conditions have been taken as representative for a medium size truck engine.

Table 1 Parameters used in the test calculations

Engine speed:	2200	1/min
Stroke	155	mm
Connecting rod	251	mm
Working gas	air	
Gas temperature at IVC	413	K
Air pressure at IVC	2.27	bar
Fuel	Methanol	
Pre-vaporized fuel	2.5%	(mass fract.)
Leanness ratio (Inv. equ. r.)	$\lambda = 1/\phi = 5.1$	
Initial droplet size (SMD)	30	µm
Initial droplet temperature	330	K
Start of injection	707.4	crank angle
Initial injection velocity	250	m/s
Gas temperature at injection	1070	K
Injection line pressure	400	bar
Nozzle hole diameter	0.3	mm

A Sauter Mean Diameter (SMD) of about 30 µm is characteristic for many technical sprays. Therefore the model predictions have been tested against independent experimental data from the literature for droplet sizes varying from 20 to 295 µm. As can be seen in Fig.2, the model calculations agree quite well with available experimental data and the known, approximately linear, initial decrease of the droplet diameter with time (d^2-law). It is also shown however, that the initial rate of vaporization

slows down for large time intervals leading to a distinct deviation of the initial linear behavior not predicted by the d^2-law (Fig. 3). This is due to (1) the droplet heating during the initial time period, (2) the strongly changing surface to volume ratio towards the end of the droplet life time, and (3) the change in liquid properties with water condensing on the droplet surface (see Fig. 12). This predictive power of the model is essential for calculating pollutant formation at late time intervals. It is concluded therefore that the fluid dynamics, the heating, and vaporization are correctly incorporated into the model.

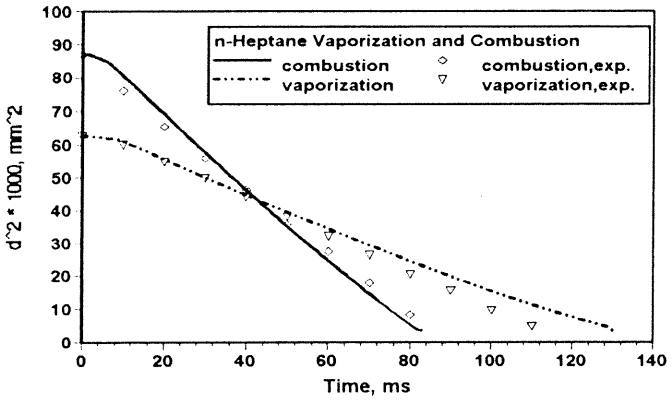

Fig. 2 Verification of the model. Comparison of calculated and experimental data [14]. T_g=1050K, T_d=300K, v_{init}=7.5 m/s, droplet diameters 295 µm and 250 µm for combustion and vaporization, resp.

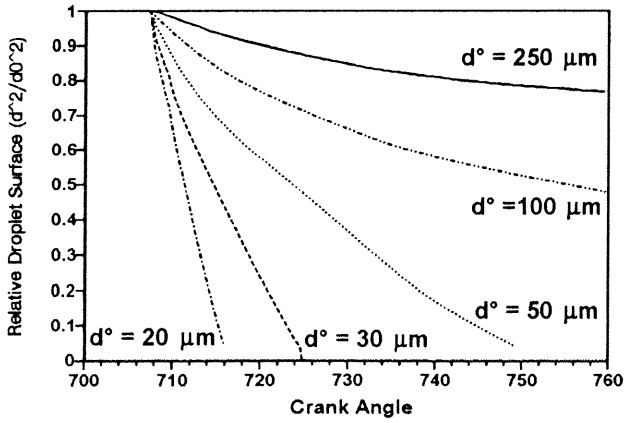

Fig. 3 Calculated variation of droplet surface, and size, with initial droplet diameter in the engine.

Ignition delay times have been used for testing the full model including the detailed reaction kinetics. The delay time is defined here as the time to a rise in gas temperature above 1500K due to chemical reactions. In the literature generally a bad prediction of ignition delay times by homogeneous kinetic models is observed at low temperatures [4-7]. This is especially true for practical combustion conditions as in engines and is sometimes explained by deficiencies in the low temperature kinetics. Therefore, an initial pool of radicals was chosen (mass fractions: $1 \cdot 10^{-4}$H, $12 \cdot 10^{-4}$O and $60 \cdot 10^{-4}$OH, corresponding to 25% of the maximum concentrations in a methanol flame [15]) and introduced into the gas phase, when detailed chemical reaction mechanisms are included. This results in reasonable ignition delays and is justified by preceding gas phase reactions due to small droplets being evaporated early on. In addition our investigations with the model showed that there is a very strong dependence of ignition delay on composition of the gas atmosphere surrounding the droplet. Further, as can be seen in Fig. 4, even small amounts of pre-evaporated fuel reduce the ignition delay drastically.

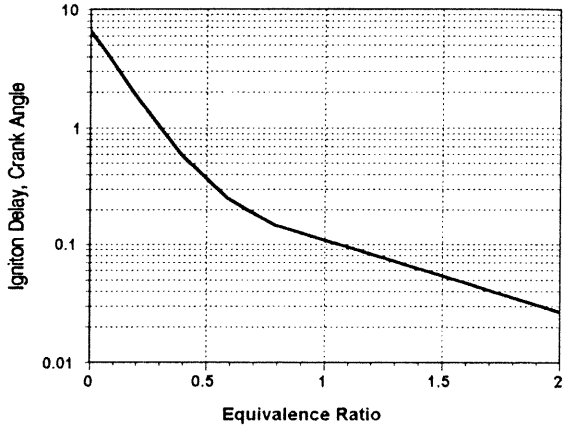

Fig. 4 Decrease in calculated ignition delay time with increasing vapor content (in terms of equivalence ratio) in the surrounding atmosphere.

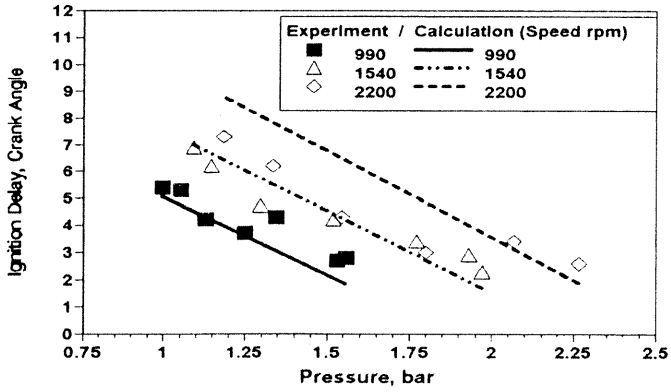

Fig. 5 Comparison of calculated and measured (in a Diesel engine) ignition delay data as function of operating conditions given in Table 2.

Table 2 Thermodynamic data of the Diesel engine used in the calculations

rpm	990	1540	2200
$p_{1,\text{full load}}$	1.56	1.97	2.27
$p_{2,\text{part load}}$	1.0	1.09	1.18
$T_{1,\text{full load}}$	357	385	413
$T_{2,\text{part load}}$	303	311	325

The reason is that reactions in the vapor phase ahead of the droplet will start immediately whereas the slow heating of the droplet and cooling of the gas by the evaporation process slow down the reactions in the vicinity of the droplet. In a real spray there is always an appreciable amount of very small droplets which will evaporate very quickly. Thus a finite vapor concentration will always be present at the ignition site effectively shortening the ignition delay time in technical systems. This plausible explanation is corroborated by a comparison of predicted ignition delay times with data obtained in a real Diesel engine (Fig.5).

In spite of the reduction of the full spray to a single droplet element a remarkable good agreement is obtained. It should be noted that 2.5% pre-vaporized fuel has been assumed in the calculation.

The same holds true for the addition of minute amounts of radicals (to the initial radical pool) as shown in Fig. 6. These radicals may come from dissociation and low temperature reactions of ignition improvers, additives, or hydrocarbons in the residual exhaust present in the combustion chamber.

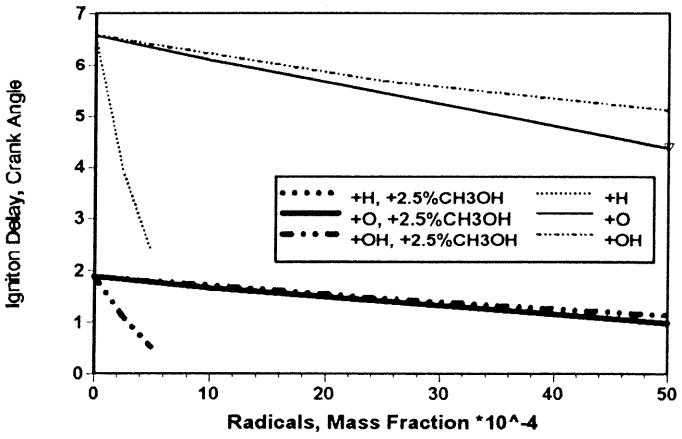

Fig. 6 Reduction of ignition delay times due to the simultaneous presence of minute amounts of radicals (in addition to the initial radical pool) and vapor in the gas.

Having verified the model against ignition delay data from real engines, details of the ignition and combustion processes were studied. By varying the droplet diameter it was revealed that there is a minimum ignition delay for a droplet diameter of about 35μm (see Fig. 7). This strikingly coincides with the mean droplet size of conventional injectors [16].

The minimum in Fig. 7 is caused by two opposing effects. The larger the droplet the smaller the surface to volume ratio and hence the less efficient the energy and mass transfer across the surface into the liquid. In spite of an increase of the absolute value of transferred energy with droplet size its relative amount drops and slows down the rate of evaporation prolonging the cooling of the vapor cloud around the droplet. Smaller droplets have a much more favorable surface to volume ratio for heating and vaporization but the resulting vapor concentrations become the lower the smaller the droplets are. According to Fig. 3, this trend increases the ignition delay time so that a minimum ignition delay time results for a specific droplet size and a given composition of the surrounding gas. The position of the minimum may be shifted by controlling the vapor concentration in the gas phase and/or the rate of vaporization.

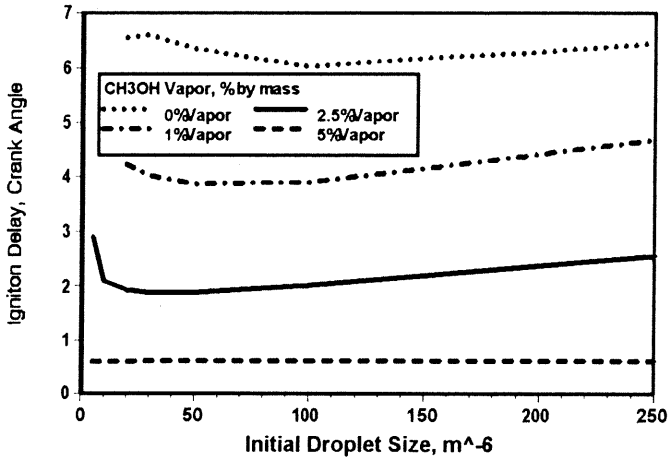

Fig.7 Position of the minimum ignition delay as function of droplet size and vapor content in the gas environment.

In Fig. 8, the effect of preheating the liquid fuel is shown. The higher the droplet temperature the lower the amount of energy required for vaporization. Thus, cooling is less pronounced, reactions proceed faster, and shorter ignition delay times result. An even stronger influence on the ignition delay time is observed if the temperature of the gas phase is varied. This is also shown in Fig. 8. This stronger effect is caused by the temperature dependence of chemical reactions in the gas phase and has to be seen also in connection with the gas phase concentrations of pre evaporated fuel and/or radicals since both - concentrations and temperature - affect reaction rates.

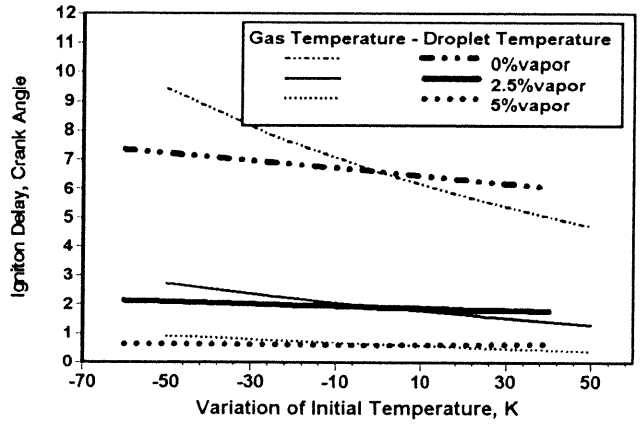

Fig. 8 Effect of fuel and gas phase temperatures on ignition delay time. Reference temperature of gas and liquid phase are 1070K and 330K, respectively.

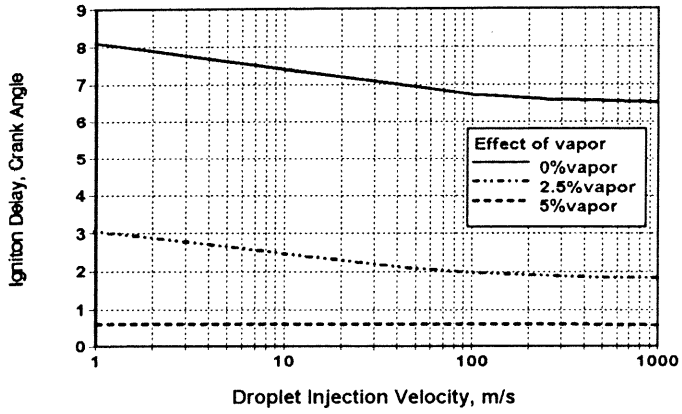

Fig. 9 Ignition delay as function of injection velocity. Initial droplet size 30μm, 0%, 2.5% and 5% pre-evaporized fuel.

Finally the effect of droplet speed on ignition delay was studied by varying the injection velocity (Fig. 9). By increasing the droplet speed, vaporization is enhanced and ignition delay drops due a higher vapor concentration surrounding the droplet (see Fig. 4)

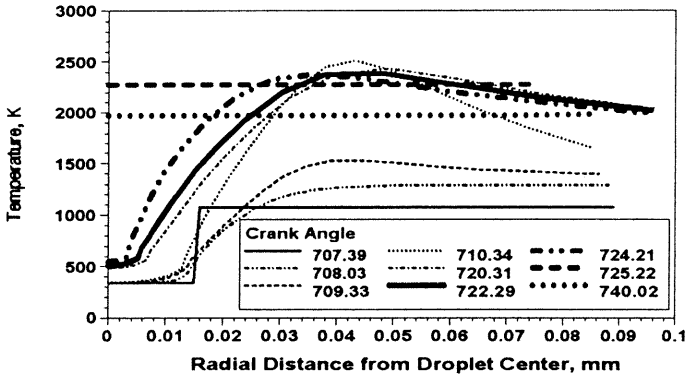

Fig. 10 Temperature distribution around a burning methanol droplet. Initial diameter 30 μm, 2.5% pre-evaporized methanol.

The temporal and spatial history of a burning 30 μm droplet is shown in Fig. 10. Initially the droplet is at 330K and the gas phase at 1070K due to gas phase reactions with the pre-evaporated fuel. In Fig. 10 the temporal evolution of droplet heating is shown exhibiting a slow increase in fluid temperature along with a shrinking of the droplet size. The critical liquid temperature (where water condensation on the droplet surface also has been taken into consideration, compare Fig. 12) is approached towards the end of the droplet life time. After the droplet is vaporized, the gas phase rapidly shows a uniform temperature distribution. In the gas phase the volume reactions develop into a broad reaction zone with peak temperatures of up to 2500K. These high gas temperatures intensify droplet heating and vaporization rates so that the reaction zone widens due to lack of oxygen. Peak temperatures start to drop. In Fig. 10 also the end of the droplet life is shown where all fuel is burned and the burned gas temperature is controlled solely by the expansion process in the engine.

These details of evaporation and combustion allow direct studies of the temporal and spatial dependencies of all concentrations in the gas phase (fuel, oxygen, products, intermediates, etc.) so that mixing and pollutant formation can be analyzed individually. As an example in Fig. 11 corresponding results are shown for the total, i.e., prompt (modified Fenimore) and thermal (extended Zeldovich), NO concentration [6,7]. NO is formed by droplet combustion (diffusion flame), approaching a temperature dependent equilibrium concentration, and subsequent reactions in the burned gas around the droplet. For clarification of the relative importance of prompt and thermal NO, the time dependent, total NO production inside a gas volume element is compared to the production of thermal NO only for a large (250μm) and a small (30μm) droplet at λ=2. In both cases, the formation of thermal NO exceeds the total NO formation. It is concluded therefore, that there exists an internal NO reduction via prompt NO mechanisms. This reduction process is enforced by large droplets providing more fuel vapor in the combustion zone.

For large droplets oxygen concentrations decrease due to increasing fuel vapor concentrations long before the end of the droplet life time. Hence, both total and thermal NO are reduced due to the concentration dependency of the chemical reactions. For small droplets, which are burning in a lean atmosphere, a significant increase in NO formation occurs after the end of their life time due to a decrease in water vapor concentration when combustion is finished.

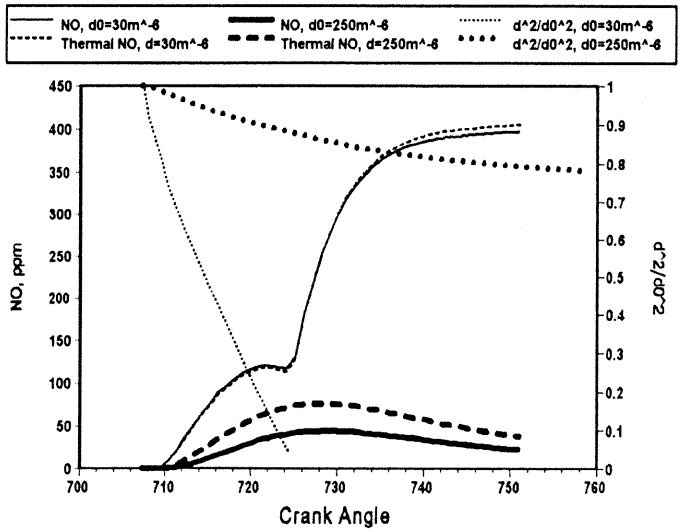

Fig. 11 Total and thermal NO formation for a small (d_1=30μm) and a large droplet (d_2=250μm) at λ=2.

Since technical fuels are mixtures of many components with different properties, the effect of different compositions of the liquid is studied by a binary mixture. Characteristic results are shown for an initially pure methanol droplet,

where a methanol/water mixture is formed by water recondensation at the droplet surface, due to the low droplet temperature. The initial air humidity (1.5 % water vapor by mass) will start the condensation process, which is accelerated after water is produced in the combustion zone. The water condensing on the droplet surface is transported towards the droplet center and evaporates near the end of the droplet life. This fractionating outside and inside a droplet is thought to be very important for understanding ignition and combustion of mixtures. In Fig.12 the distribution of the water fraction around and inside a combusting droplet is shown.

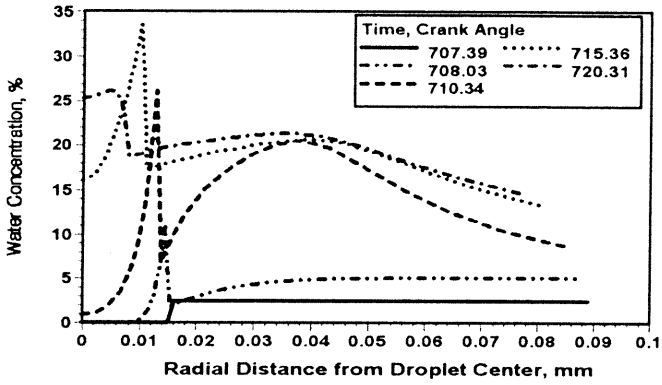

Fig. 12 Spatial water distribution (molar concentrations) - water vapor in the gas phase, condensed liquid water inside the droplet, initially at 30 μm.

CONCLUSIONS

A spray element containing only a single droplet under relevant gas phase conditions has been shown to characterize fundamental spray behavior even in engines. Mixing, combustion and pollutant formation may be studied in detail.

Ignition is improved and ignition delay time is reduced even by small amounts of prevaporized fuel and/or radicals in the gas phase surrounding a droplet.

An increase in the initial gas temperature reduces the ignition delay time more than an increase in initial fuel temperature.

There exists a minimum ignition delay time for a certain droplet diameter, in the present study for droplets sized between 30 and 50 μm. The location of the minimum may be influenced by the vapor concentration in the gas phase and the temperatures of gas and liquid phase, respectively.

Prompt NO formation must be included in pollutant predictions since it influences the internal reburn process, rendering inclusion of thermal NO formation alone insufficient.

REFERENCES

1. Law, C.K., "Recent Advances in Droplet Vaporization and Combustion", Prog. Energy Combust. Sci., Vol. 8, pp. 171-201, 1982.

2. Sirignano, W.A., "Fuel Droplet Vaporization and Spray Combustion Theory", Prog. Energy Combust. Sci., Vol. 9, pp. 291-322, 1983.

3. Dwyer, H.A., "Calculations of Droplet Dynamics in High Temperature Environments", Prog. Energy Combust. Sci., Vol. 15, pp. 131-158, 1989.

4. Warnatz, J., "Resolution of Gas Phase and Surface Combustion Chemistry into Elementary Reactions", 24th Symp. (Int.) on Combustion, Vol. , pp. 553-579 , 1992.

5. Warnatz, J. and Chevalier, C., "Critical Survey of Elementary Reaction Rate Coefficients in the C/H/O System", in W.C. Gardiner jr. (ed.), Combustion Chemistry, 2nd edition, Springer Verlag, New York, 1993.

6. Bockhorn, H., Chevalier, C., Warnatz, J., Weyrauch, V., "Experimental Investigation and Modeling of Prompt NO Formation in Hydrocarbon Flames", HDT 166, Heat Transfer in Fire and Combustion Systems, p.111, 1991.

7. Thorne, L.R., Branch, M.C., Chandler, D.W., Kee, R.L, Miller, J.A., "Hydocarbon/Nitric Oxide interactions in Low-Pressure Flames", 21st Symp. (Int.) on Combustion, The Combustion Institute, pp.965-977, 1986.

8. Dwyer, H.A. and Sanders, B.R., "Calculations of Unsteady Reacting Droplet Flows", 22nd Symp. (Int.) on Combustion, The Combustion Institute, pp.1923-1929, 1988.

9. Kee, R.J., Rupley, F.M. and Miller, J.A., "CHEMKIN II, A Fortran Chemical Kinetics Package for the Analysis of Gas-Phase Chemical Kinetics", Sandia Report SAND89-8009, 1990.

10. Westbrook, C.K., Dryer, F.L., "Chemical Kinetic Modeling of Hydrocarbon Combustion", Prog. Energy Combust. Sci., Vol.10, pp.1-57, 1984.

11. Reid, R.C., Prausnitz, J.M. and Poling, B.E., "The Properties of Liquids and Gases", 4th edition, Mc Graw-Hill, New York, 1987.

12. Stapf, P., "Modellierung der Tröpfchenverbrennung unter Einschluß detaillierter chemischer Reaktion", Dissertation, Universität Stuttgart, 1993.

13. Stull, D.R., Westrum, E.F. and Sinke, G.C., "The Chemical Thermodynamics of Organic Compounds", Wiley, New York, 1969.

14. Lee, A. and Law, C.K., "An Experimental Investigation on the Vaporization and Combustion of Methanol and Ethanol Droplets", Combust. Sci. and Tech., Vol. 86, pp.253-265, 1992.

15. Vandooren, J., Van Tiggelen, P.J., "Experimental Investigation of Methanol Oxidation in Flames: Mechanisms and Rate Constants of Elementary Steps", 18th. Symp. (Int.) on Comb., pp.473-483, 1981.

16. Maly, R.R., Mayer, G., Reck, B., Schaudt, R.A., Optical diagnostics for Diesel-Sprays with ms-Time Resolution, SAE paper 910727, 1991.